Chaotic Dynamics Near Triple Collision

RICHARD MOECKEL

Communicated by R. MCGEHEE

Introduction

Perhaps the simplest solutions of the three-body problem are the periodic orbits discovered by LAGRANGE in 1772 [L]. Three masses arranged in an equilateral triangle can rotate uniformly around their center of mass if the rate of rotation is chosen so that the centrifugal force just balances the gravitational attraction. These orbits are part of a family of periodic orbits in which the triangle formed by the masses remains equilateral but varies in size as each mass traverses an ellipse. For each fixed energy and angular momentum there are two such Lagrangian elliptical orbits (up to rotation) corresponding to the two distinct orderings of the masses around the triangle.

Besides the equilateral triangles, there are three other configurations which admit such simple motions. For each of the three distinct orderings of the masses along a line there is a unique choice of spacing giving rise to uniformly rotating solutions. These also lie in a family of elliptical orbits called Eulerian since EULER discovered how to choose the spacing [Eu].

As the angular momentum approaches zero the ellipses degenerate to line segments and the periodic solutions approach solutions exhibiting triple collisions in both forward and backward time. It is known that, for certain choices of the masses, the Lagrangian circular orbits are stable. It turns out, however, that for sufficiently small angular momenta the Lagrangian elliptical orbits are always unstable. This suggests the possibility of solutions homoclinic to one of the Lagrange orbits or heteroclinic between the two of them. The existence of such orbits is one of the main results of this paper (Theorem 4).

In addition to the Lagrangian orbits we can construct a variety of other periodic orbits exhibiting close approaches to triple collision. Among them are orbits which approximate all five Lagrangian and Eulerian elliptical motions in succession between their close approaches to collision (Theorem 3). Figure 9 shows one of the many possible behaviors. These new periodic orbits are linked with each other and with the Lagrangian orbits in a complicated network of homoclinic and heteroclinic connections. The whole network is described by use of symbolic dynamics.

We obtained results similar to these in a special case of the three-body problem where a symmetry is used to lower the number of degrees of freedom [M1]: the isosceles three-body problem reduces to a flow on a three-dimensional manifold. The planar problem unfolds in five dimensions. The stable and unstable manifolds of the Lagrangian elliptical orbits are each three-dimensional and we are looking for transverse intersections. The strategy is to study first the case of zero angular momentum and then to treat the case of small nonzero angular momentum as a perturbation.

Using the scaling technique of MCGEHEE to tame the triple collision singularity we find that as the angular momentum tends to zero, the Lagrangian orbits converge to a restpoint cycle (Figure 2). The stable and unstable manifolds of the restpoints patch together to form the stable and unstable sets of the cycle. These are again three-dimensional. We are able to produce intersections of these limiting sets by the following technique. The restpoints corresponding to the Lagrangian orbits are connected to restpoints corresponding to the Eulerian orbits. For certain choices of the masses, the latter exhibit complex eigenvalues. As the stable and unstable manifolds of the Lagrangian restpoints pass by they are wound into spirals around the Eulerian orbits and are thereby forced to intersect one another. Some of the details regarding spiralling of invariant manifolds in high dimensions are treated in [M2]. After constructing these intersections in the zero angular momentum case we study the effect of the perturbation to nonzero angular momenta, obtaining the results described above.

Two interesting questions remain open. First, we may wonder whether the homoclinic orbits to Lagrange's orbits persist for fairly large angular momenta. We mentioned above that for certain masses, the circular Lagrange orbits are stable; however, for other masses, including the case of exactly equal masses, these orbits are still hyperbolic. For such masses it is possible that homoclinic orbits exist over the whole range of angular momenta. Second, we may ask whether the invariant set described above is part of a larger invariant set which also includes oscillation and capture phenomena. This is so in the simpler isosceles case [M1]. In the planar problem the behavior of orbits "near infinity" is more complicated and we have not been stable to incorporate them into the symbolic dynamics.

1. Three-body problem in the plane

Let $m_k > 0$ be the masses of point particles with positions $q_k \in \mathbb{R}^2$ and momenta $p_k \in \mathbb{R}^2$; $k = 1, 2, 3$. Let $q, p \in \mathbb{R}^6$ denote the vectors (q_1, q_2, q_3), (p_1, p_2, p_3). The three-body problem is governed by the Hamiltonian function

$$H(p, q) = \tfrac{1}{2} p \cdot A^{-1} p - U(q)$$

where A is the 6×6 mass matrix diag $(m_1, m_1, m_2, m_2, m_3, m_3)$, $\cdot$ is the scalar product in $\mathbb{R}^6$, and

$$U(q) = \frac{m_1 m_2}{|q_1 - q_2|} + \frac{m_1 m_3}{|q_1 - q_3|} + \frac{m_2 m_3}{|q_2 - q_3|}.$$

Hamilton's equations are

$$\dot{q} = A^{-1}p,$$
$$\dot{p} = \nabla U(q).$$

We will assume that the center of mass remains at the origin:

$$m_1q_1 + m_2q_2 + m_3q_3 = 0,$$
$$p_1 + p_2 + p_3 = 0.$$

Let $r = (q \cdot Aq)^{\frac{1}{2}}$, the square root of the moment of inertia. Note that $r = 0$ if and only if all three masses collide at the origin. McGEHEE introduced the substitutions $s = r^{-1}q$, $z = r^{\frac{1}{2}}p$, $' = r^{\frac{1}{2}}$ which lead to the equations

$$\begin{aligned} r' &= vr, \\ s' &= A^{-1}z - vs, \\ z' &= \nabla U(s) + \tfrac{1}{2}vz \end{aligned} \tag{1.1}$$

where $v = s \cdot z$ [Mc]. Replacing q by the pair (r, s) is analogous to the introduction of polar coordinates. The normalized position vector s describes the shape of the triangle formed by the three particles while r describes its size. The vector s lies on a five-dimensional ellipsoid in $\mathbb{R}^6$ defined by

$$s \cdot As = 1. \tag{1.2}$$

In these coordinates, the assumption about the center of mass gives

$$\begin{aligned} m_1s_1 + m_2s_2 + m_3s_3 &= 0, \\ z_1 + z_3 + z_3 &= 0. \end{aligned} \tag{1.3}$$

Solutions with energy $H(p, q) = h$ satisfy

$$H(z, s) = \tfrac{1}{2}z \cdot A^{-1}z - U(s) = rh. \tag{1.4}$$

For solutions with angular momentum $p \times q = \sum_{n=1}^{3} p_k \times q_k = \omega$ we have

$$r^{\frac{1}{2}}(z \times s) = \omega. \tag{1.5}$$

In this paper we will study certain solutions of the planar three-body problem which have negative energy $(h < 0)$ and small angular momentum ($|\omega|$ small). Let

$$M(h, \omega) = \{(r, s, z) : r \geqq 0,\ s \notin \Delta,\ 1.2\text{–}1.5 \text{ hold}\}$$

where $\Delta = \{s : s_i = s_j \text{ for some } i \neq j\}$. The structure of M depends on the masses as well as on h and ω.

The topology of $M(h, \omega)$ can best be understood by considering the projection to the configuration space. Let $\Sigma = \{s : s \notin \Delta,\ 1.2\text{–}1.3 \text{ hold}\}$. The equations 1.2 restrict s to a four-dimensional plane in $\mathbb{R}^6$ and 1.3 then determines a three-dimensional ellipsoid in this plane. The collision set, Δ, breaks up into three com-

ponents corresponding to the three equations $s_1 = s_2$, $s_1 = s_3$, and $s_2 = s_3$. Within the ellipsoid these give three circles, each of which is linked with the other two. Thus the configuration space Σ is a three-dimensional ellipsoid with three circles deleted.

The projection map $(r, s, z) \to s$ restricts to a map $\Pi: M(h, \omega) \to \Sigma$. For the energies and angular momenta we want to study, this map has a simple structure. It is surjective and the fiber over any point of Σ is diffeomorphic to the three-dimensional sphere S^3. In fact, the following result can be proved [Sm]:

Proposition 1.1. *There is a constant $C < 0$ depending only on the masses such that for $C < h\omega^2 < 0$ the manifold $M(h, \omega)$ is diffeomorphic to $\Sigma \times S^3$.*

It follows that for any given $h < 0$ the conclusion of the proposition holds for $|\omega|$ sufficiently small.

It is important to note that the three-body problem possesses rotational symmetry, Let $R(\theta)$ denote the 6×6 block diagonal matrix with blocks

$$\begin{pmatrix} \cos\theta & -\sin\theta \\ \sin\theta & \cos\theta \end{pmatrix}.$$

Then $(r(t), s(t), z(t))$ solves 1.1 if and only if $(r(t), Rs(t), Rz(t))$ does. This means that the vectorfield 1.1 determines a vectorfield on the quotient space of $M(h, \omega)$ under the action of the rotation group. This space is easily seen to be $\tilde{\Sigma} \times S^3$ where $\tilde{\Sigma}$ is the quotient space of Σ under the action. $\tilde{\Sigma}$ is diffeomorphic to a two-dimensional sphere with three deleted points, one for each of the deleted circles of Σ (Figure 1).

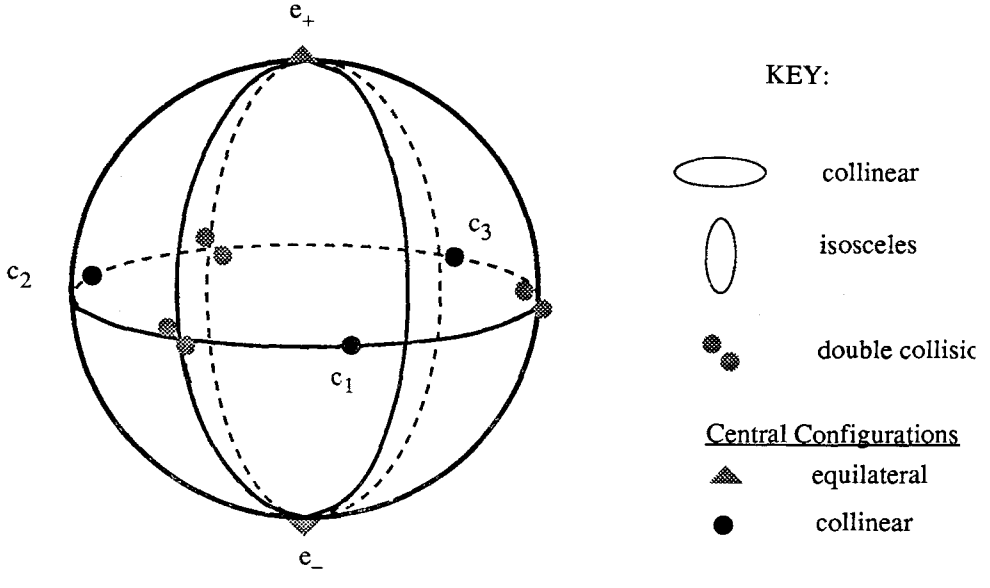

Fig. 1

The rotational symmetry leads to the construction of the periodic solutions of EULER and LAGRANGE. These are solutions which exhibit configurations of constant shape. More precisely, let $s \in \Sigma$ be a fixed configuration. We seek a solution of 1.1 with $s(t) = R(\theta(t))\, s$. In other words the normalized configuration changes only by a rotation; we allow the size of the configuration (described by $r(t)$) to change arbitrarily. Substitution into 1.1 leads to the following equation:

$$(v' - (\theta')^2 - \tfrac{1}{2} v^2)\, As + (\theta'' + \tfrac{1}{2} v\theta')\, AJs - \nabla U(s) = 0$$

where J is the 6×6 block diagonal matrix with blocks $\begin{pmatrix} 0 & -1 \\ 1 & 0 \end{pmatrix}$. If we take the scalar product of this equation with s and with Js we find (using $\nabla U(s) \cdot s = -U(s)$ and $\nabla U(s) \cdot Js = 0$):

$$v' = (\theta')^2 + \tfrac{1}{2} v^2 - U(s),$$

$$\theta'' + \tfrac{1}{2} v\theta' = 0.$$

With these equations in hand the original equation becomes

$$\nabla U(s) = -U(s)\, As. \tag{1.6}$$

If we set $\alpha = \theta'$ the other equations are

$$\begin{aligned} v' &= \alpha^2 + \tfrac{1}{2} v^2 - U(s), \\ \alpha' &= -\tfrac{1}{2} v\alpha. \end{aligned} \tag{1.7}$$

Equation 1.6 concerns the constant configuration vectors. A solution is called a central configuration. Up to rotation there are just five central configurations in the three-body problem [S-M]. For each of the three rotationally inequivaent ways to order the three particles in a line there is a unique collinear central configuration. These are called the Eulerian central configurations [Eu]. The exact spacing of the particles depends in a complicated way on the masses. In addition, each of the two rotationally inequivalent arrangements of the masses in an equilateral triangle is a central configuration. These are the Lagrangian configurations [L]. Note that equation 1.6 implies that at a central configuration, the gradient of U is normal to the ellipsoid $s \cdot As = 1$. Thus central configurations can be viewed as critical points of the restriction of U to this ellipsoid. Figure 1 depicts the quotiented configuration space $\tilde{\Sigma}$ with the central configurations. We have labelled the collinear central configurations $c_j, j = 1, 2, 3$, where j is the subscript of the mass which lies between the other two. The equilateral configurations are e_+ and e_-.

Once a central configuration, $s = s_0$, has been found, equations 1.7 determine the corresponding solutions of the three-body problem. The size $r(t)$ can be found using the energy and angular momentum equations

$$\tfrac{1}{2}(v^2 + \alpha^2) - U(s_0) = rh,$$

$$r^2\alpha = \omega.$$

Fixing $h < 0$ leads to the phase portrait of Figure 2 in the (r, v)-plane. The family of periodic orbits is parametrized by $|\omega|$. The rest point $r = U(s_0)/|h|$, $v = 0$ corresponds to $\omega^2 = \frac{1}{2} U_0^2/|h|$. For larger angular momenta there are no motions possible. As $|\omega|$ decreases we pass through the family of periodic motions to the restpoint cycle, which corresponds to $\omega = 0$. Note that this cycle contains two restpoints and a connecting orbit in $\{r = 0\}$, the triple collision set. Orbits in the collision set do not represent actual motions of the three-body problem but rather additional motions of system 1.1. As can be seen from Figure 2, however, they do reflect the behavior of actual orbits passing close to triple collision.

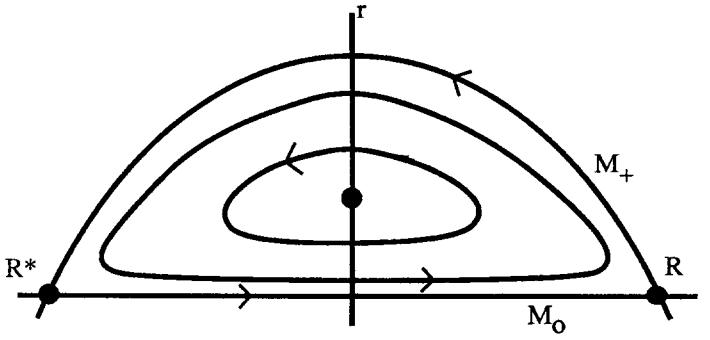

Fig. 2

It is interesting to ask how the positions of the three particles vary along these periodic orbits. It turns out that each particle follows an elliptical path according to Kepler's laws. The family of periodic orbits corresponding to an equilateral central configuration is shown in Figure 3. The central restpoint in our phase portrait has $r(t)$ constant and so corresponds to the circular orbit in Figure 3. The portion of the restpoint cycle with $r > 0$ repreents an orbit which begins and ends in triple collision and corresponds to the radial motion in Figure 3

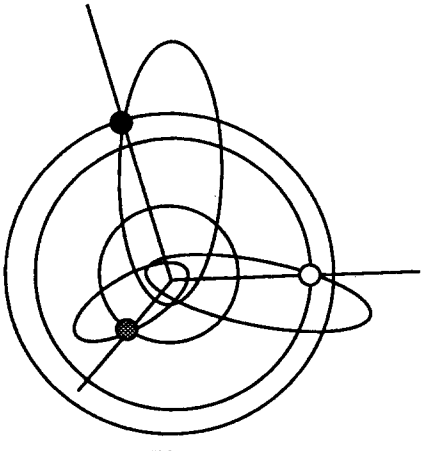

Fig. 3

which is the limiting behavior of elliptical motion as the eccentricity tends to 1. It is interesting to note that along the other branch of the cycle (invisible in Figure 3) one computes a change in θ of exactly 2π radians, so even in the limit the normalized configuration rotates once as we go around the cycle.

We now see that each quotiented manifold $\tilde{M}(h, \omega)$ with $h < 0$ and $0 < |\omega|$ sufficiently small contains five simple periodic orbits, corresponding to the five central configurations. These are important landmarks in the flow. As noted above, their existence goes back to EULER and LAGRANGE. The local structure of these orbits, at least in the nearly circular case, has been well-studied [S-M]. The goal of this paper is to show that for $|\omega|$ sufficiently small, these five orbits are part of an intricate invariant set which also includes many other periodic orbits as well as orbits homoclinic to them and heteroclinic between them. The method we employ is to first study the case $\omega = 0$, where the periodic orbits are replaced by restpoint cycles, and then view the case of small angular momentum as a perturbation.

2. Zero angular momentum

From now on we fix an energy $h < 0$. We will write $M(\omega)$ instead of $M(h, \omega)$ to denote the integral manifolds described above. As there is no loss of generality in considering only non-negative angular momenta, we consider what happens to $M(\omega)$ as $\omega \to 0+$. As can be seen already in Figure 2 the manifolds develop "corners" as they approach the collision set $\{r = 0\}$.

Let $M(0+) = \{(r, s, z) : r \geqq 0, s \notin \Delta,$ 1.2–1.5 hold, $z \times s \geqq 0\}$, where in 1.5 we are to set $\omega = 0$. We will use just M instead of $M(0+)$ to simplify notation. Clearly 1.5 now factors into two equations $r = 0$ or $z \times s = 0$. Let M_0 be the subset of M where $r = 0$ and M_+ the subset where $z \times s = 0$. M_+ is just the $\omega = 0$ integral manifold of the three-body problem. M_0, on the other hand, lies entirely in the triple collision set and so contains no actual solutions of the three-body problem. Let $C = M_+ \cap M_0$. C is called the triple collision manifold and it forms a boundary for the $\omega = 0$ integral manifold [Mc1]. Orbits in C reflect the behavior of actual zero angular momentum solutions of the three-body problem which pass close to triple collision. As we saw in Section 1, orbits in M_0 reflect the behavior of non-zero angular momentum solutions which pass close to triple collision. In Figure 2, the restpoints in the restpoint cycle lie in C, the top connecting orbit lies in $M_+ \setminus C$ and the bottom connecting orbit lies in $M_0 \setminus C$.

$M = M_+ \cup M_0$ is the union of two manifolds-with-boundary, glued together along their common boundary, C. M_+ and M_0 meet at a corner so M is not a smooth manifold. However it is not difficult to prove the following result.

Proposition 2.1. *M_+ and M_0 are diffeomorphic to $\Sigma \times D^3$, where D^3 is a closed three-dimensional disk. The collision manifold $C = M_+ \cap M_-$ is the common boundary $\Sigma \times S^2$. $M = M_+ \cup M_0$ is homeomorphic to $\Sigma \times S^3$.*

The corner at C does not present much of a problem for the dynamics since M_+, M_0 and C are invariant under equations 1.1. As $\omega \to 0+$, the differentiable

manifolds $M(\omega)$ (also homeomorphic to $\Sigma \times S^3$ by Proposition 1.1) converge to M just as the elliptical periodic orbits converged to the restpoint cycle in Figure 2.

We now turn to the study of the flow on M. A good deal is known about the flow on M_+, including its boundary, C [D1, M3, S, W]. The flow on $M_0 \setminus C$ has not yet been investigated. We will only discuss features relevant to the goal of the paper.

The vectorfield 1.1 restricted to M_0 is gradient-like with respect to $v = s \cdot z$. In fact, an important inequality due to SUNDMAN can be written [M3]:

$$v' \geqq rh + \tfrac{1}{2}(z \times s)^2 .$$

On M_0 we have $r = 0$ and $z \times s \geqq 0$ with equality only on C. Thus $v' > 0$ on solutions in $M_0 \setminus C$. A closer analysis shows that even in C, $v(t)$ is increasing on every non-constant solution. This means that the restpoints are especially important.

We have already found ten restpoints in C, namely, two in each of the five restpoint cycles. Actually, because of the rotational symmetry there are ten circles of restpoints in C. One verifies from 1.1 that there are no other restpoints. For reference we record the coordinates of the restpoints:

$$\begin{aligned} r &= 0, \\ s &= s_0 \text{ (central configuration)}, \\ v &= \pm(2U(s_0))^{\frac{1}{2}}, \\ z &= vAs_0 . \end{aligned} \tag{2.1}$$

To label the restpoints, let E_+ and E_+^* denote the restpoints corresponding to the central configuration e_+, where the star indicates the choice of a minus sign in 2.1. Similarly we use E_-, E_-^*, C_j, C_j^* to represent the other restpoints. Figure 4 shows the levels of the restpoints with respect to the non-decreasing function v.

All ten restpoints are hyperbolic when viewed in the quotient manifold of C under the rotational symmetry. The eigenvalues are closely related to the behavior of the potential near the corresponding central configuration. The variational equations of 1.1 involve the second derivative of the potential function. Let $\tilde{U}: \tilde{\Sigma} \to \mathbb{R}$ be the restriction of the potential to the quotiented configuration space and let $\tilde{\nabla}$ be the gradient operator with respect to the metric induced on $\tilde{\Sigma}$ by the metric A on $\mathbb{R}^6$. Then $D\tilde{\nabla}\tilde{U}(s_0)$ will have two (real) eigenvalues. It turns out that if λ is such an eigenvalue then

$$\frac{v \pm \sqrt{v^2 + 16\lambda}}{4} \tag{2.2}$$

is an eigenvalue of the variational matrix at the corresponding restpoint [D2]. Here v is given by 2.1.

Now e_+ and e_- are non-degenerate minimum of $\tilde{U}$ while c_j are non-degenerate saddle points. From this one can easily work out the dimensions of the stable and

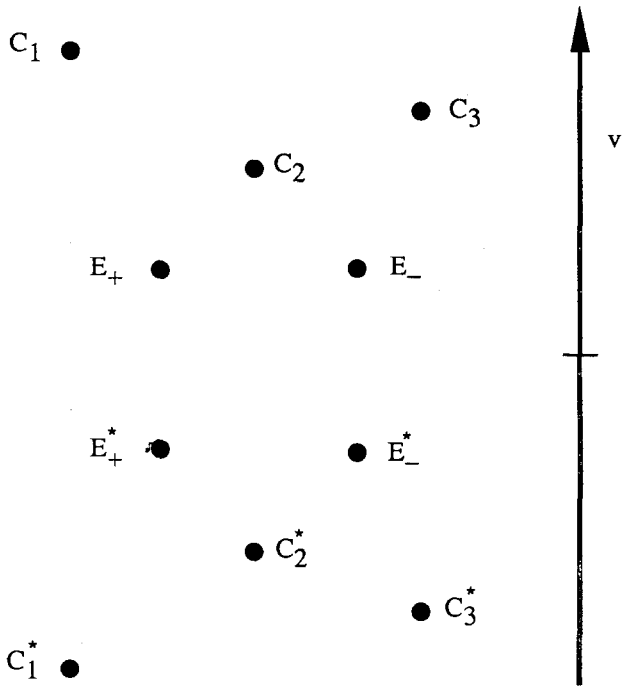

Fig. 4

unstable manifolds in C of each restpoint. These are shown in Table 1 along with the exact values of the eigenvalues. The latter were obtained from the intricate computation in [S-M] by a change of time scale.

Since $\mu \geqq 0$, the eigenvalues at the equilateral restpoints are always real. Note that for equal masses, $\mu = 0$ and so the eigenvalues occur with multiplicity two. From 2.2 it follows that the two eigenvalues of $D\,\tilde{\nabla}\tilde{U}(e_{+,-})$ agree in this case; this fact will be useful later on.

To understand fully the eigenvalues at the collinear restpoints we need to know the spacing of the masses along the line (determined by α, β). These satisfy $\frac{1}{\alpha} + \frac{1}{\beta} = 1$ and

$$\frac{m_i\alpha\beta + m_j\beta}{m_i + m_j\beta^2} = \frac{m_k\alpha\beta + m_j\beta}{m_k + m_j\alpha^2}.$$

As noted above, there is a unique solution α, β for given m_1, m_2, m_3. It turns out that there is a large open set of masses such that $\nu_j > \frac{1}{8}$ which makes two of the stable eigenvalues at C_j and two of the unstable eigenvalues at C_j^* complex. Since this is crucial in what follows we will describe this set of masses. When $m_i = m_k = m$, $\alpha = \beta = \frac{1}{2}$ and one finds easily that $\nu_j > \frac{1}{8}$ if and only if $\frac{m}{m_j} > \frac{4}{55}$. In particular, for equal masses, all six collinear restpoints exhibit complex eigenvalues. Figure 5 shows the regions in the mass simplex $m_1 + m_2 + m_3 = 1$ where the various ν_j exceed $\frac{1}{8}$. [R-S.]

Table 1. Eigenvalues at the restpoints in C

Restpoint R	dim $St(R)$	dim $Un(R)$	Eigenvalues $\left(\lvert v\rvert = \sqrt{2U(R)}\right)$
$E_{+,-}$	2	2	$-\frac{\lvert v\rvert}{4} 1 \pm \left(\sqrt{13 \pm 12\sqrt{\mu}}\right)$
$E^*_{+,-}$	2	2	$\frac{\lvert v\rvert}{4}\left(1 \pm \sqrt{13 \pm 12\sqrt{\mu}}\right)$
C_j	3	1	$-\frac{\lvert v\rvert}{4}\left(1 \pm \sqrt{1 \pm \sqrt{25 + 16v_j}}\right)$, $-\frac{\lvert v\rvert}{4}\left(1 \pm \sqrt{1 \pm \sqrt{1 - 8v_j}}\right)$
C^*	1	3	$\frac{\lvert v\rvert}{4}\left(1 \pm \sqrt{1 \pm \sqrt{25 + 16v_j}}\right)$, $\frac{\lvert v\rvert}{4}\left(1 \pm \sqrt{1 \pm \sqrt{1 - 8v_j}}\right)$

$$\mu = \frac{(m_1 - m_2)^2 + (m_1 - m_3)^2 + (m_2 - m_3)^2}{2(m_1 + m_2 + m_3)^2},$$

$$v_j = \frac{m_i(1 + \alpha + \alpha^2) + m_k(1 + \beta + \beta^2)}{m_i + m_j(\alpha^2 + \beta^2) + m_k},$$

$$\alpha = \frac{r_{ik}}{r_{ij}}, \quad \beta = \frac{r_{ik}}{r_{jk}} \quad \{i,j,k\} = \{1,2,3\}.$$

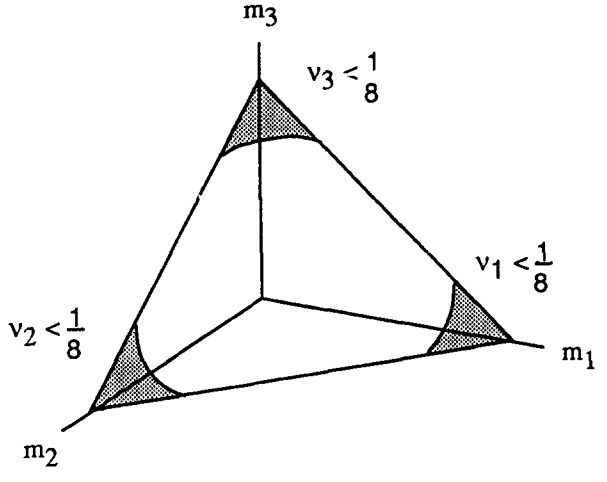

Fig. 5

We now turn to the behavior of the restpoints in the direction complementary to C in M. Recall that M is composed of two pieces M_0 and M_+ which meet at a corner along C. As indicated in Figure 2 the restpoints exhibit different behaviors in these pieces. Each starred restpoint has an additional stable eigenvalue in M_+ and an additional unstable eigenvalue in M_0. The situation is reversed at each unstarred restpoint. This unusual state of affairs results from our viewing the restpoint in the manifold with corners M rather than from any degeneracy of the restpoint itself.

The fact that the dimensions of both the stable and unstable sets of the restpoints are increased when we view the restpoints in M is crucial to our perturbation strategy. Consider the restpoint cycle corresponding to one of the Lagrangian central configurations, e_+ or e_-. In $\tilde{M}_+$, the quotient space of M_+ under the symmetry, the restpoint E has a three-dimensional unstable manifold and E^* has a three-dimensioal stable manifold. Since $\tilde{M}_+$ is five-dimensional it is dimensionally possible that the restpoint connection in the cycle represents a transverse intersection of these stable and unstable manifolds. In fact, this is the case for all choices of the masses [D2, S-L]. In $\tilde{M}_0$ E^*, has a three-dimensional unstable manifold and E has a three-dimensional stable manifold. Thus it is dimensionally possible for the other branch of the restpoint cycle to be a transverse connection. This is also true, at least for generic masses. The proof will be given in Section 4.

Proposition 2.2. *For all masses the Lagrangian connecting orbit* $E_{+,-} \to E^*_{+,-}$ *is transverse. For generic masses the connecting orbit* $E^*_{+,-} \to E_{+,-}$ *in the collision set is transverse.*

Here generic means that the exceptional masses lie in the zero set of an analytic function on the mass space. In particular, the set of allowable masses is open and dense and has full measure.

Because of the transversality of the connecting orbits, the unstable manifolds of $E_{+,-}$ and $E^*_{+,-}$ fit together to give an unstable topological manifold for the restpoint cycle. Similarly there is a patchwork stable manifold for the cycle. In the quotiented spare $\tilde{M}$ these objects are three-dimensional. This hyperbolic structure of the restpoint cycle carries over to the nearby periodic orbits in the manifolds $M(\omega)$. Thus we have:

Proposition 2.3. *Let the masses be so chosen that both connecting orbits of the restpoint cycle are transverse. Then for all sufficiently small angular momenta,* ω, *the Lagrangian periodic orbits in* $\tilde{M}(\omega)$ *are hyperbolic with three-dimensional stable and unstable manifolds.*

Since $\tilde{M}(\omega)$ is five-dimensional it is possible to have transverse homoclinic or heteroclinic orbits connecting the two Lagrangian periodic orbits.

The Eulerian periodic orbits are apparently not hyperbolic. The restpoint cycles corresponding to collinear central configurations are not transverse, as a glance at Table 1 will show. In $\tilde{M}_+$, C_j has a two-dimensional unstable manifold while C_j^* has a two-dimensional stable manifold. Thus the existence of the connect-

ing orbit $C_j \to C_j^*$ seems surprising. The explanation is that both of these manifolds are contained in a three-dimensional invariant submanifold of $\tilde{M}_+$, namely, the collinear invariant manifold. If we start the three bodies on a line with momenta parallel to the line, then they will remain collinear for all time. These motions form a three-dimensional subsystem of $\tilde{M}_+$ which contains the stable and unstable manifolds of the collinear restpoints [Mc2]. Viewed in this invariant manifold, the $C_j \to C_j^*$ connection is transverse [D2].

We now turn to the construction of homoclinic and heteroclinic orbits to the Lagrangian orbits. First we consider the case of zero angular momentum. As we remarked above, the stable and unstable manifolds of $E_{+,-}$ and $E_{+,-}^*$ patch together to give stable and unstable manifolds for the Lagrangian restpoint cycle. We will show that for certain choices of the masses these manifolds intersect each other transversely infinitely often. The Eulerian orbits play a crucial role in the proof of this claim; they are brought into play by means of the following result [M3]:

Proposition 2.4. *For all masses, topologically transverse connecting orbits of the following types occur in the collision manifold, C:*

$$\left.\begin{aligned} E_{+,-} &\to C_j \\ C_j^* &\to E_{+,-}^* \end{aligned}\right\} \quad j = 1, 2, 3.$$

Because of these connecting orbits, parts of the unstable manifolds of $E_{+,-}$ pass near each collinear restpoint C_j. Similarly the stable manifolds of $E_{+,-}^*$ pass near C_j^* in backward time. The implications of these facts in the case when the collinear restpoints have complex eigenvalues can be seen schematically in Figure 6. Figure 6 is actually taken from a subsystem of the planar three-body problem which occurs when two of the three masses are equal. In that case, initial conditions which are symmetrical under reflection through some line lead to solutions which remain symmetrical for all time. This subsystem is called the isosceles three-body problem and has been extensively studied [D1, M1, M4, S]. If the particle with subscript j is on the axis of symmetry (the other two being the equal masses) then the restpoints $E_{+,-}$, $E_{+,-}^*$, C_j and C_j^* lie in the isosceles submanifold together with parts of their stable and unstable manifolds. These are depicted in the figure. The main point is that the spiralling near the collinear restpoints causes the asymptotic manifolds of the equilateral restpoints to wind themselves around the $C_j \to C_j^*$ connecting orbit and thus produces infinitely many transverse intersections.

We will see that this mechanism still works in the full planar three-body problem. The main difficulty is the higher dimension of the various manifolds. In Figure 6 we have two-dimensional asymptotic manifolds in a three-dimensional space. In the planar problem we have (after removing the rotational symmetry) three-dimensional asymptotic manifolds in a five-dimensional space. An advantage of the planar problem is that we now have three collinear restpoints which, for certain choices of the masses, all exhibit spiralling.

The first step in the construction is to clarify what it means for one invariant

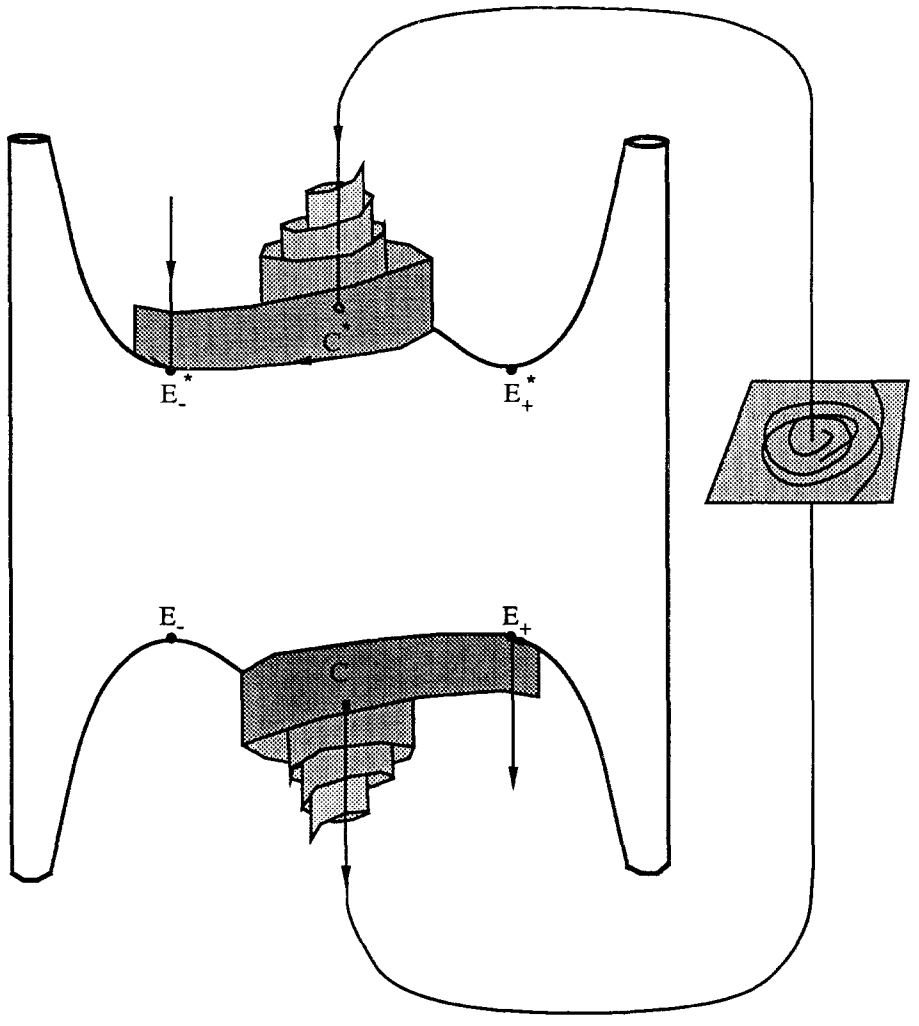

Fig. 6

manifold to spiral around another. We have developed some of the theory of spirals in another paper [M2] and will present only a summary here. The concept of spiralling presupposes a codimension-two submanifold around which the spiralling takes place. For example, a curve can spiral around a point in a plane or around another curve in space. A surface may also be said to spiral around a curve in space (see Figure 7). In the isosceles problem, the $C_j \to C_j^*$ connecting orbit provides the required codimension-two submanifold. In the planar problem we need a three-manifold. The natural choice is the collinear subsystem mentioned above; it is a codimension-two subsystem of the full planar problem and it contains the $C_j \to C_j^*$ connection.

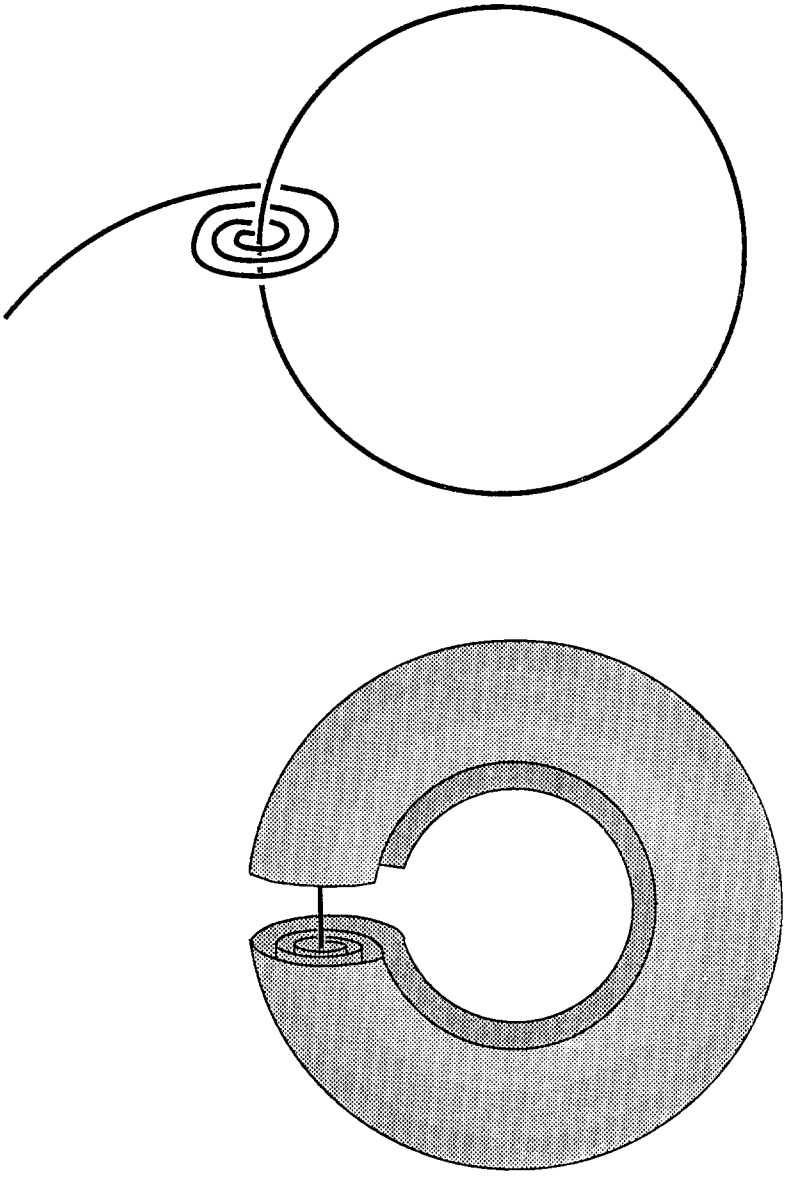

Fig. 7

Given a codimension-two submanifold we can define what it means for another manifold to spiral around it. Locally, one can introduce polar coordinates in the complementary two dimensions; this can even be done globally if the submanifold is nicely embedded. A spiralling manifold should wind around the submanifold and converge to it as the angular coordinate tends to ∞ (or to $-\infty$). We require that the spiral converge in a controlled way. First of all, it must approach a definite submanifold of the codimension-two manifold; we call this the core of the spiral.

In Figure 7 one spiral has a point as its core and the other has a circle as its core. The spiral itself should consist of a one-parameter family of copies of the core manifold, parametrized by the angular coordinate. As this parameter tends to $\pm\infty$, the copies of the core should converge smoothly to the core itself. Various technical conditions assure that in any other polar coordinate system we can still find such a parametrization [M2].

Spirals of this kind are formed near hyperbolic restpoints of flows when complex eigenvalues are present. Consider the situation near a collinear restpoint C_j when the masses are chosen so as to have complex eigenvalues. In the quotiented manifold $\tilde{M}_+$ (five-dimensional) we find the invariant three-dimensional collinear submanifold containing the restpoint and its unstable manifold. The complex eigenvalues are stable ones and the complex eigenspace is a complement to the collinear manifold. The complete stable manifold is three-dimensional since there is also a real stable eigenvalue in the collinear manifold. If we take a small two-dimensional disk transverse to the stable manifold then according to [M2] it emerges from a neighborhood of the restpoint as a manifold spiralling around the invariant collinear manifold and converging to the unstable manifold of the restpoint (the core). This situation can be visualized if we consider a four-dimensional cross-section to the flow near some point of the unstable manifold of the restpoint (Figure 8). In this cross-section the collinear manifold appears as a co-dimension-two submanifolds; *i.e.*, as a two-dimensional surface. Within this surface the unstable manifold of the restpoint appears as a curve. If we choose a polar coordinate system in the complementary dimensions and then fix the angular coordinate we get a three-dimensional half-space bounded by the collinear manifold. This is pictured in the figure. The image of the transversal disk is wound around the collinear manifold in such a way that it intersects the half-space in

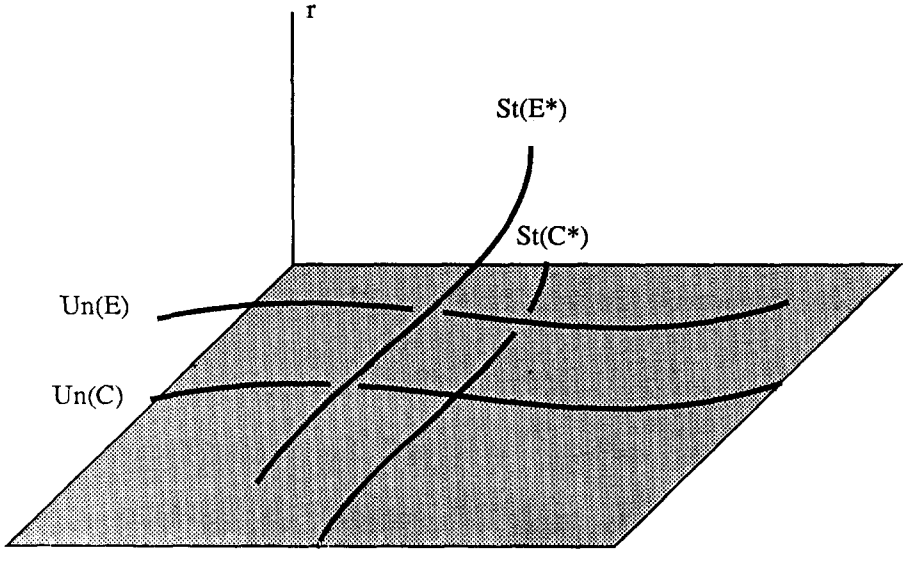

Fig. 8

a curve which lies over the unstable manifold of the restpoint. As the angular coordinate is varied the curves converge to the core curve, the unstable manifold of the restpoint.

We want to find a complementary two-dimensional disk to the stable manifold of C_j which lies in the unstable manifold of E_+ or E_-. According to Propositions 2.3 we can find disks which are topological complements. Of course it is to be expected that for generic masses, the connecting orbits described by the proposition are actually transverse but this has not been proved. Unfortunately the results of [M2] require transversality. It is possible to establish transversality for special choices of the masses. The following result will be proved in Section 4.

Proposition 2.5. *If the masses m_1 and m_2 are sufficiently close to being equal then there are transverse connecting orbits $C_3^* \to E_{+,-}^*$ and $E_{+,-} \to C_3$ in the collision manifold. The same is true if the subscripts 1, 2, 3 are permuted.*

The proposition is proved by considering the connecting orbits in the isosceles submanifolds for the case when two masses are equal (Figure 6). Clearly this connection is transverse in the isosceles submanifold. By studying the variational equations in the directions complementary to the isosceles manifold one can show that these connections are transverse when viewed in the full planar manifold. The proposition then follows since transversality is preserved by small perturbations.

Thus for appropriately chosen masses $Un(E_+)$ and $Un(E_-)$ each contain disks which pass near the collinear restpoint C_j and emerge as spirals around the collinear invariant manifold with core $Un(C_j)$.

Consider a four-dimensional cross-section to the flow along the $C_j \to C_j^*$ connecting orbit. Recall that when viewed in the collinear manifold this orbit represents a transverse intersection of $Un(C_j)$ and $St(C_j^*)$. Thus in Figure 8 we find these manifolds as transverse curves in the collinear manifold. By following two-dimensional disks in $St(E_{+,-}^*)$ and $St(E_\pm^*)$ in backward time through a neighborhood of C_j^* we find similar spirals converging to $St(C_j^*)$. These spiral in the opposite sense to the spirals arising from $Un(E_{+,-})$: if the "unstable" spirals converge to their cores as the angular coordinate tends to $+\infty$, then the "stable" spirals converge as the angular coordinate tends to $-\infty$. Then it is clear from Figure 8 that there will be intersections of the unstable curves and the stable curves as the angular coordinate is varied. From the results in [M2] it follows that in every neighborhood of $Un(C_j) \cap St(C_j^*)$ there are infinitely many topologically transverse intersections of each of $Un(E_{+,-})$ with each of $St(E_{+,-}^*)$.

Theorem 1. *Let the masses be chosen so that the restpoints C_j and C_j^* have complex eigenvalues and so that the connections $E_{+,-} \to C_j$ and $C_j^* \to E_{+,-}^*$ are transverse. Then in every neighborhood of the $C_j \to C_j^*$ connection there are topologically transverse connections from each of $E_{+,-}$ to each of $E_{+,-}^*$.*

Our main interest in this result is its implications for the Lagrange orbits with small but non-zero angular momenta. However we have the following result for the zero angular momentum problem.

Corollary. *For masses as in the theorem there are infinitely many solutions of the three-body problem which both begin and end in triple collision. As they approach collision their configurations approach an equilateral triangle; however, such orbits occur in every neighborhood of the collinear orbit* $C_j \to C_j^*$.

This phenomena was first found by DEVANEY in the isosceles problem [D1].

For the perturbation theory in the next section, it is convenient to introduce a graph representing the various restpoint connections in M.

Definition. For each mass vector m and energy $h < 0$, the *connection graph* $G(m, h)$ is the directed multigraph with four vertices E_+, E_-, E_+^*, E_-^* and one directed edge between vertices for each topologically transverse connecting orbit between the corresponding restpoints in the flow on the limiting variety $M(h)$.

With this terminology, Proposition 2.2 and Theorem 1 can be combined as follows:

Theorem 1'. *Let the masses be chosen so that the restpoints* C_j *and* C_j^* *have complex eigenvalues and so that the connections* $E_{+,-} \to C_j$ *and* $C_j^* \to E_{+,-}^*$ *are transverse. Then for any* $h < 0$, *the connection graph* $G(m, h)$ *contains the graph*:

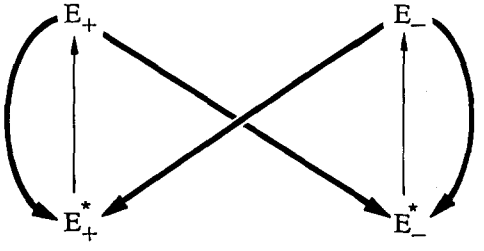

(2.3)

where the bold arrows indicate a countable infinity of distinct edges. Moreover, connections of the type represented by the bold arrows occur in every neighborhood of the Eulerian $C_j \to C_j^*$ *connecting orbit.*

In this graph, each upward-pointing arrow represents the branch of a Lagrangian restpoint cycle which lies in M_0. The branch in M_+ is represented by one of the semicircular arrows. The other arrows represent connections caused by the spiralling near the Eulerian restpoints C_j and C_j^*. Note that the hypotheses may be satisfied for several values of j in which case the bold arrows get even bolder. Also, the complete connection graph may contain other edges unrelated to the ones found in this section. In particular there may be other connections from $E_{+,-}^* \to E_{+,-}$ in M_0 besides the one in our Lagrangian restpoint cycle. The perturbation theorem of the next section applies to those orbits, if they exist.

3. Nonzero angular momentum

In the first section of this paper we found that the Lagrangian elliptical periodic orbits in $M(h, \omega)$ converge as $\omega \to 0$ to restpoint cycles in the limiting variety M. In the second section we constructed infinitely many other orbits in M connecting the same restpoints; these were represented as edges in the connection graph. Now we will see what happens to this collection of restpoint connections when we return to nonzero angular momenta.

The results are best described using symbolic dynamics in the quotient manifolds $\tilde{M}(h, \omega)$. Along each of the orbits in the connection graph we erect a small transversal or "window". Since all $\tilde{M}(h, \omega)$ are homeomorphic to $\tilde{M}$ and converge to $\tilde{M}$ as $\omega \to 0$ we can erect corresponding windows in $\tilde{M}(h, \omega)$ and these will still be transverse to the flow for small $|\omega|$. Thus we can view the edges of the connection graph as representing windows in $\tilde{M}(h, \omega)$ instead of orbits in $\tilde{M}$. We will say that a path in the graph is realized by an orbit if the orbit crosses all of the windows corresponding to the edges in the path in the order described by the path. A path may be bi-infinite. We can choose the windows so as to make the following theorem true.

Theorem 2. *Let Γ be a finite subgraph of the connection graph $G(m, h)$. There is a positive constant $\omega(\Gamma)$ such that for $0 < |\omega| < \omega(\Gamma)$, the flow on $\tilde{M}(h, \omega)$ realizes every path in Γ.*

This result and its proof are essentially higher dimensional versions of those in a previous paper [M1]. Before discussing the proof we turn to the corollaries. As in [M1], cycles in the graph lead to periodic orbits in the flow; the proof of the following is omitted.

Proposition 3.1. *Let Γ be a finite subgraph of $G(m, h)$ and let $0 < |\omega| < \omega(\Gamma)$. If C is a cycle in Γ then the set $I(C)$ of orbits realizing C is a compact isolated invariant set which carries a one-form; moreover $I(C)$ contains at least one periodic orbit.*

For a discussion of "carrying a one-form" see [C]. It is likely that the set $I(C)$ consists in a single unstable periodic orbit. We can verify this for the special cycles representing the Lagrangian periodic solutions. Let l_0 be the edge in C corresponding to the $E_+^* \to E_+$ branch of our restpoint cycle and let l_+ be the $E_+ \to E_+^*$ branch. Then the path $\ldots l_0 l_+ l_0 l_+ \ldots$ is a cycle and the Lagrangian periodic orbit realizes it. Since this orbit is known to be hyperbolic we can choose the windows corresponding to l_0, l_+ in such a way that no other orbit can realize the cycle. Similarly the other Lagrangian periodic orbit is the unique orbit realizing a certain cycle. If the masses are chosen so that Theorem 1′ holds then there are infinitely many other cycles in G. It is interesting to consider the qualitative behavior of the triangle formed by the three bodies along the corresponding periodic orbits. All cycles in the graph 2.3 repeatedly traverse the two vertical arrows. These represent windows close to triple collision. The behavior is near that along the branch of the Lagrangian restpoint cycle; namely the particles form a tiny triangle which

is nearly equilateral and spin around through an angle of nearly 360 degrees. The downward pointing arrows represent behaviors between these close approaches to collision. Among the possible behaviors we have the behaviors of the Lagrangian and Eulerian restpoint cycles. In other words, the particles can emerge from their close approach near an equilateral configuration or nearly collinear. We can therefore construct periodic orbits which mimic the behavior of these famous orbits in virtually any order we like. If the masses are so chosen that Theorem 1′ holds for $j = 1, 2, 3$ (for example, nearly equal masses) then all five of the central configurations can be incorporated. Such orbits, which follow the Lagrangian and Eulerian periodic orbits except near the close approaches, can also be aperiodic. We want to be a bit more precise about how well we can approximate these behaviors. Let $Z = \{v = 0\}$. The branches of the Lagrangian and Eulerian restpoint cycles which lie in $\tilde{M}_+$ cross Z at unique points. If we recall that $r' = v$ we see that by intersecting with Z we are catching these orbits just as the moment of intertia (size) of the configuration reaches its maximum. The windows we will construct to prove Theorem 2 will lie in Z. There are no windows around the points where the Eulerian orbits hit Z but there are windows in every neighborhood of them. We can arrange that the orbits we construct follow an arbitrary compact piece of the Lagrangian or Eulerian orbits with arbitrary accuracy by requiring that they hit Z sufficiently close to these points. This can be done by specifying windows.

Theorem 3. *Let arbitrary neighborhoods of the Lagrangian and Eulerian ejection-collision orbits be given. Suppose the masses are nearly equal. Then for sufficiently small angular momenta there are orbits that pass through the given neighborhoods in any order and that satisfy the following selection rule: passes through neighborhoods of different Lagrangian orbits must be separated by at least one pass through an Eulerian neighborhood. If the sequence of neighborhoods is periodic then there is a periodic orbit realizing it.*

This follows from Theorems 1′ and 2. Figure 9 shows the behavior of a periodic orbit constructed in this way.

If C_1 and C_2 are cycles in Γ we can construct orbits heteroclinic between $I(C_1)$ and $I(C_2)$ by choosing a path $\gamma \in \Gamma$ whose backward tail agrees with C_1 and whose forward tail agrees with C_2. Choosing the cycles corresponding to the Lagrangian periodic orbits we have:

Theorem 4. *For small angular momenta there exist orbits homoclinic to the Lagrangian elliptical orbits and heteroclinic between them. Such orbits can be found near the Eulerian elliptical periodic orbits.*

There is another way to prove Theorem 4 which does not involve symbolic dynamics and which provides some transversality. We know that the Lagrangian restpoint cycles have three-dimensional stable and unstable sets in $\tilde{M}$ and that the Lagrangian periodic orbits have three-dimensional stable and unstable manifolds in $\tilde{M}(h, \omega)$. Furthermore, the asymptotic manifolds of the cycle have infinitely many topologically transverse intersections. The same would hold for the periodic orbits if we knew that the asymptotic manifolds behaved smoothly as $\omega \to 0$.

It is possible to carry out this program in spite of the fact that the limiting manifolds are not smooth but have corners at the restpoints. We will not pursue this line of reasoning here.

By choosing the cycles C_1 and C_2 in other ways we can find orbits which are homoclinic to or heteroclinic between the periodic orbits of Theorem 3 (or at least the corresponding sets I). For example there are orbits asymptotic to a Lagrangian elliptical orbit in backward time and to orbits behaving as in Figure 9 in forward time.

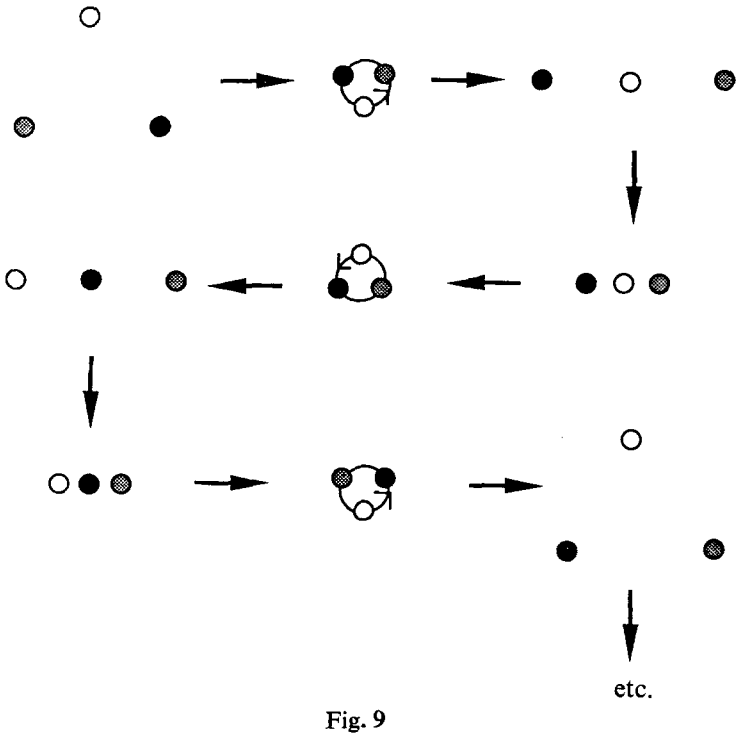

Fig. 9

We turn now to proof of Theorem 2. We will develop a four-dimensional special case of window theory [E]. Let $I = [-1, 1]$ and $I^n = [-1, 1] \times \ldots \times [-1, 1]$, the n-dimensional cube. Viewing I^4 as $I^2 \times I^2$ we define certain subsets of the boundary: $\partial_+ = \partial I^2 \times I^2$ and $\partial_- = I^2 \times \partial I^2$. Each of these is a solid torus and $\partial I^4 = \partial \cup \partial_-$.

We will use the terminology of singular homology theory. A relative two-chain σ which represents a non-zero class in the relative homology group $H_2(I^4, \partial_+) \simeq \mathbb{Z}$ will be called a positive chain. Similarly we can define negative chains. The following simple fact underlies much of what follows.

Proposition 3.2. *Let K be a compact subset of I^4 which is disjoint from ∂_+ but which intersects every positive chain. Let L be compact, disjoint from ∂_- and intersecting every negative chain. Then $K \cap L \neq \emptyset$.*

Proof. Consider the triple $(I^4, I^4 \setminus K, \partial_+)$. A portion of the exact cohomology sequence of this triple is:

$$\longrightarrow H^2(I^4, I^4 \setminus K) \xrightarrow{i^*} H^2(I^4, \partial)_+ \xrightarrow{j^*} H^2(I^4 \setminus K, \partial_+) \longrightarrow$$

where i and j are inclusion maps.

Let α_+ be a cocycle representing a generator of $H^2(I^4, \partial_+)$. Then α_+ vanishes when applied to any relative cycle which is not positive. Let σ be any relative cycle for the pair $(I^4 \setminus K, \partial_+)$. By hypothesis, $j(\sigma)$ cannot be a positive chain in (I^4, ∂_+). Therefore $\alpha_+(j(\sigma)) = j^*\alpha_+(\sigma) = 0$. By the exactness of the sequence, $\alpha_+ = i^*z_+$ for some $z_+ \in H^2(I^4, I^4 \setminus K)$. Similarly, if α_- generates $H^2(I^4, \partial_-)$ then $\alpha_- = i^*z_-$ with $z_- \in H^2(I^4, I^4 \setminus L)$.

Now suppose $K \cap L = \emptyset$. Then the cup product $z_+ \cup z_- \in H^4(I^4, I^4 \setminus (K \cap L)) = H^4(I^4, I^4)$ will vanish. But $i_*(z_+ \cup u_-) = \alpha_+ \cup \alpha_- \in H^4(I^4, \partial I^4)$ is a generator, a contradiction. Hence $K \cap L \neq \emptyset$.

A window for a flow on a five-dimensional manifold $\tilde{M}$ is an embedding $w: I^4 \to \tilde{M}$ such that $w(I^4)$ is transverse to the flow. We sometimes write $(w, \partial\pm)$ instead of $(w(I^4), w(\partial\pm))$ in what follows. Given windows w_0 and w_1 it may happen that there is a Poincaré map defined on some part of w_0 mapping into w_1. We will define a notion of correct alignment of windows, meant to capture the idea that the flow stretches w_0 across w_1 in some way. Our definition is different from that in [E]. To the windows w_0, w_1 we associate auxiliary windows W_0, W_1 with $W_0 \cap W_0(\partial_+) = W_1 \cap w_1(\partial_-) = \emptyset$. Let $\Delta_+ = W_1 \setminus w_1$ and $\Delta_- = W_0 \setminus w_0$. We require the existence of retractions $r_0: (W_0, \Delta_-) \to (w_0, \partial_-)$ and $r_1: (W_1, \Delta_+) \to (w_1, \partial_+)$ inducing isomorphisms in homology (see Figure 10).

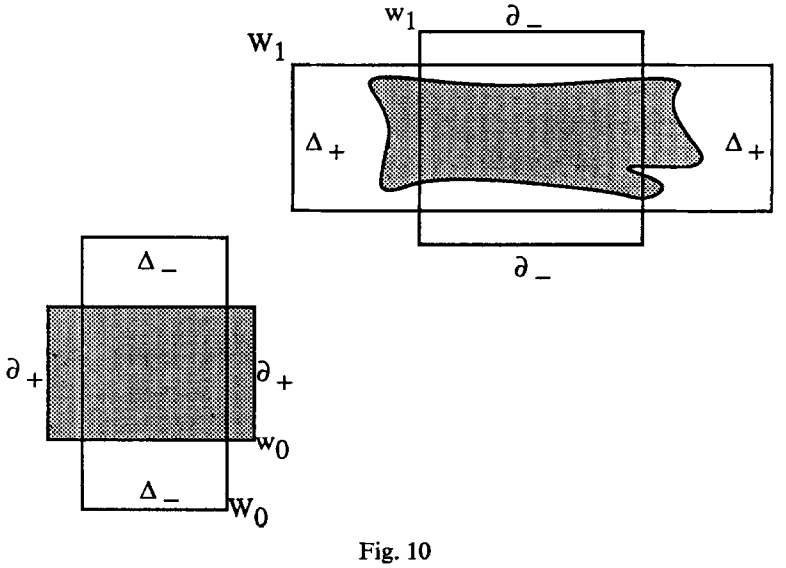

Fig. 10

Definition. w_0 and w_1 are correctly aligned if there are Poincaré maps $\varphi : (w_0, \partial_+) \to (W_1, \Delta_+)$ and $\psi : (w_1, \partial_-) \to (W_0, \Delta_-)$ inducting isomorphisms in homology.

Several remarks are in order. The main difficulty with Poincaré maps is finding their domain and range. Note that $\hat{\varphi} = r_1 \circ \varphi : (w_0, \partial_+) \to (w_1, \partial_+)$ and $\hat{\psi} = r_0 \circ \psi : (w_1, \partial_-) \to (w_0, \partial_-)$ are defined on the whole window and that for any point p with $\hat{\varphi}(p) \in \text{int}\,(w_1)$, $\hat{\varphi}(p) = \varphi(p)$ since the retraction r_1 fixes w_1 and takes Δ_+ to ∂_+. Similarly, if $\hat{\psi}(q) \in \text{int}\,(w_0)$ then $\hat{\psi}(q) = \psi(q)$. The condition for correct alignment has the advantage that is depends only on the action of the flow on $w_0(\partial_+)$ and $w_1(\partial_-)$; in fact, a simple exact sequence argument shows that the windows are correctly aligned if and only if $\varphi_* : H_*(\partial_+) \to H_*(\Delta_+)$ and $\psi_* : H_*(\partial_-) \to H_*(\Delta_-)$ are isomorphisms. This makes it easy to verify correct alignment.

Now let $w_0, w_1, \ldots, w_N$ be a sequence of windows correctly aligned by a flow and let $\varphi_1, \ldots, \varphi_N$ be the Poincaré maps. The composition $\varphi_N \circ \ldots \circ \varphi_1$ will be defined on some compact subset D_N of w_0 whose properties we now investigate.

Lemma. *Let σ be any positive chain in w_0. Then $|\sigma| \cap D_N \neq \emptyset$.*

Proof. $|\sigma|$ denotes the image of the chain σ, which is a relative two-chain repesenting a nonzero homology class in $H_2(w_0, \partial_+)$. The composition $\hat{\varphi}_N \circ \ldots \circ \hat{\varphi}_1$, is defined on all of w_0 and induces an isomorphism of $H_2(w_0, \partial_+)$ and $H_2(w_N, \partial_+)$. Consequently the image chain $\hat{\varphi}_N \circ \ldots \circ \hat{\varphi}_1(\sigma)$ represents a nonzero class in the latter group. It follows that $\hat{\varphi}_N \circ \ldots \circ \hat{\varphi}_1(|\sigma|)$ intersects the interior of w_N; if not then since it is disjoint from ∂_-, it lies in ∂_+ and so is trivial in $H_2(w_N, \partial_+)$. Let $q \in \hat{\varphi}_N \circ \ldots \circ \hat{\varphi}_1(|\sigma|) \cap \text{int}\,(w_N)$ say, $q = \hat{\varphi}_N \circ \ldots \circ \hat{\varphi}_1(p)$ where $p \in |\sigma|$. Then $q = \varphi_N \circ \ldots \circ \varphi_1(p)$ and $p \in |\sigma| \cap D_N$ as required.

Proposition 3.3. *Let $\ldots, w_{-N}, \ldots, w_0, \ldots, w_N, \ldots$ be a sequence of windows correctly aligned by a flow. Then there is a nonempty, compact subset of w_0 whose forward orbits pass through $w_1, w_2, \ldots$ and whose backward orbits pass through $w_{-1}, w_{-2}, \ldots$ under the appropriate Poincaré maps.*

Proof. The domain of definition of $\varphi_N \circ \ldots \circ \varphi_1$, D_N, intersects every positive chain in w_0. Dually, the domain of the backward Poincaré map $\psi_{-N} \circ \ldots \circ \Psi_1$, D_N^*, intersects every negative chain in w_0. Applying Proposition 3.2 we have $D_N \cap D_N^* \neq \emptyset$ for all N. Since these sets are nested, $\bigcap_N D_N \cap D_N^*$ is nonempty and compact.

Let α be one of the orbits represented by the edges in the connection graph. Then α is a topologically transverse intersection of the stable and unstable manifolds of two equilateral restpoints, say $St(E)$ and $Un(E')$. We will work in the five-dimensional space $\tilde{M}$ where these manifolds have dimension three. Let Z be a transversal to α at some point p. If α is one of the orbits from graph 2.3 we can always choose $Z = \{v = 0\}$, as noted above. Since p is a topologically transverse intersection of $St(E) \cap Z$ and $Un(E') \cap Z$, we can choose C^0 local coordinates $U \to \mathbb{R}^4$, where U is a neighborhood of p in Z, taking p to 0, $Un(E')$ to $\mathbb{R}^2 \times 0$

and $St(E)$ to $0\times\mathbb{R}^2$. The window associated to α will be a small cube in this coordinate system.

Under the flow on $\tilde{M}$ such a window can be followed forward to a neighborhood of E where it accumulates on the unstable manifold of E. Similarly, in backward time the window accumulates on $St(E')$. Suppose that β is an orbit corresponding to a connection $E \to E''$. Then following the window of α forward and the window of β backward brings them both in to the neighborhood of E. Recalling the unusual nature of the flow near E (Figure 11) we see that the windows are stretched in a favorable way and brought quite close together. However, the flow on $\tilde{M}$ cannot correctly align the windows since necessarily one window is in $\tilde{M}_+$ and the other is in $\tilde{M}_0$, and these are separated by the invariant collision manifold C. It happens that when we perturb to nonzero angular momenta, the restpoint disappears and the windows are correctly aligned. We will carry out the proof of this assertion in two steps. First we show that the windows along α and z are correctly aligned with windows in the boundary of a small ball around E. Then we show that these new windows are correctly aligned by the flows on $\tilde{M}(h, \omega)$ for $|\omega|$ sufficiently small. Both steps are greatly facilitated by the construction of a good coordinate system near E.

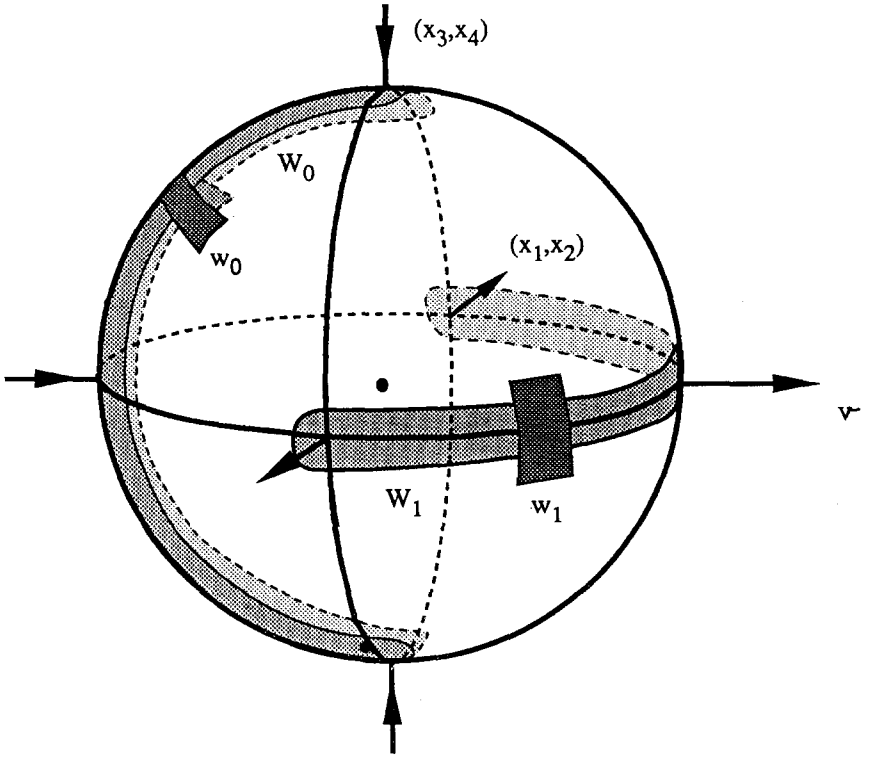

Fig. 11

First we set $z = vAs + \Omega AJs + w$ where $v = z \cdot s$, $\Omega = zxs = z \cdot Js$ and w is defined by the equation. The new differential equations are:

$$r' = vr,$$
$$s' = \Omega Js + A^{-1} w,$$
$$v' = \tfrac{1}{2} v^2 + \Omega^2 + w^T A^{-1} w - U(s),$$
$$\Omega' = -\tfrac{1}{2} v\Omega,$$
$$w' = \nabla U(s)_t - \tfrac{1}{2} vw - \Omega Jw - (w^T A^{-1} w)\, As.$$

Here $\nabla U(s)_t = \nabla U(s) + U(s)\, As$, the component of $\nabla U(s)$ tangent to the ellipsoid $s^T As = 1$. The energy and angular momentum equations become:

$$\tfrac{1}{2}(v^2 + \Omega^2 + w^T A^{-1} w) - U(s) = rh,$$
$$r^{1/2}\Omega = \omega.$$

The first of these two equations can be used to eliminate v locally near E, since $v(E) \neq 0$. With this accomplished we have only the equation $r\Omega^2 = \omega^2$. Now let $\mu = 2|h| r\Omega^2$ and $\nu = |h| r - \Omega^2$. Then (μ, ν, s, w) provide C^0 local coordinates near E which are smooth away from C but have the effect of flattening the corner at E. To see this, just note that the constraint equation becomes simply $\alpha = |h| \omega^2$. In particular, M corresponds to $\{\alpha = 0\}$. Now the differential equations for α, z are easily found:

$$\mu' = 0,$$
$$\nu' = v\sqrt{\mu^2 + \nu^2}.$$

Here $v(\mu, \nu, s, w)$ is obtained from $v(r, s, \Omega, w)$ by substitution. Since E is hyperbolic in the directions complementary to ν in $\tilde{M}$ we obtain the following lemma:

Lemma 3.4. *There are coordinates $(\nu, x_1, \ldots, x_4)$ near E in $\tilde{M}$ in which the vector-field takes the form:*

$$\nu' = |v(E)| \cdot |\nu| + \ldots,$$
$$x_j' = \lambda_j x_j + \ldots$$

where $\lambda_1 \geqq \lambda_2 > 0 > \lambda_3 \geqq \lambda_4$ are the eigenvalues of E in C. Moreover $C = \{\nu = 0\}$, $St(E) = \{\nu \leqq 0, x_1 = x_2 = 0\}$ and $Un(E) = \{\nu \geqq 0, x_3 = x_4 = 0\}$. These coordinates can also be used in the nearby manifolds $\tilde{M}(h, \omega)$ and then the equations depend continuously on ω with $\nu' = |v(\nu, x)| \sqrt{h^2\omega^4 + \nu^2}$.

This follows from the discussion above, replacing ν by $-\nu$ if $v(E) < 0$. Figure 11 shows a schematic picture of the flow near E in these coordinates. As mentioned above the effect of the perturbation to nonzero angular momenta is to eliminate the restpoint and render $\nu' > 0$ so that the obstruction to correct alignment of our windows is removed.

We have said that the window associated to the connecting orbit α, $E' \to E$, is to be a cube in a special coordinate system set up on the transversal Z to α. This coordinate system takes $St(E)$ and $Un(E')$ into coordinate planes. The last lemma provides us with special coordinate systems near the restpoints E, E'. In particular, if B is a small ball around E and if $q = \alpha \cap \partial B$ then there is some neighborhood of q on which the vectorfield points strictly into B and on which $(x_1, \ldots, x_4)$ will serve as local coordinates. Similarly there are coordinates $(x_1', \ldots, x_4')$ near the point $q' = \alpha \cap \partial B'$ where B' is a small ball around E'. We may assume that the vectorfield points out of B' on a neighborhood of q'. Finally let $(y_1, \ldots, y_4)$ denote the coordinates near p in Z. The next lemma shows that by choosing the window w_0 in Z appropriately we can be sure that w_0 is correctly aligned with windows $w_{-1} \subset \partial B'$ and $w_1 \subset \partial B$ which are cubes in their respective coordinate systems. The maps φ_{-1} and φ_1 in the lemma represent the Poincaré maps from the neighborhood in $\partial B'$ into Z and from Z into the neighborhood in ∂B, respectively. The maps in the lemma are only assumed to be C^0 because y was only a C^0 coordinate system. Finally, the preservation of $\mathbb{R}^2 \times 0$ and $0 \times \mathbb{R}^2$ by φ_{-1} and φ_1 correspond to the invariance of $Un(E')$ and $St(E)$ under the Poincaré maps.

Lemma. *Let* $x = \varphi_1(y)$ *and* $y = \varphi_{-1}(x')$ *be local homeomorphisms of* $(\mathbb{R}^4, 0)$ *such that* φ_1 *preserves* $0 \times \mathbb{R}^2$ *and* φ_{-1} *preserves* $\mathbb{R}^2 \times 0$. *Then there are windows* w_{-1}, w_0, w_1 *which are cubes in* x', y, x *coordinates, respectively, such that* φ_{-1} *correctly aligns* w_{-1} *and* w_0 *and* φ_1 *correctly aligns* w_0 *and* w_1.

Proof. Let $\|(\xi, \eta)\| = \max(|\xi|, |\eta|)$ be the square metric on $\mathbb{R}^2$. Write $x = (\bar{x}, \bar{\bar{x}})$ with $\bar{x} \in \mathbb{R}^2 \times 0$ and $\bar{\bar{x}} \in 0 \times \mathbb{R}^2$ and do the same for x' and y.

We may assume that the maps restrict to homeomorphisms on the unit cube in y space. Consider the squares $\|\bar{\bar{y}}\| = 1$ and $\|\bar{\bar{y}}\| = b < 1$ in $0 \times \mathbb{R}^2$. If b is sufficiently small then their φ_1 images can be separated by a square of the form $\|\bar{\bar{x}}\| = f$. Similarly we can choose $0 < a < 1$ so that the φ_{-1} preimages of $\|\bar{y}\| = 1$ and $\|\bar{y}\| = a$ can be separated by a square $\|\bar{x}'\| = c$. Let $w_0 = \{\|\bar{y}\| \leqq a, \|\bar{\bar{y}}\| \leqq b\}$ and let $W_0^+ = \{\|\bar{y}\| \leqq a, \|\bar{\bar{y}}\| \leqq 1\}$ and $W_0^- = \{\|\bar{y}\| \leqq 1, \|\bar{\bar{y}}\| \leqq b\}$ (see Figure 12). Actually these do not quite work as auxiliary windows since, for example, $W_0^+ \cap \partial_- \neq \emptyset$. But later we can shrink W_0^+ a little in the $\bar{y}$ direction and W_0^- a little in the $\bar{\bar{y}}$ direction.

For the rest of the proof we can work with φ_1 and φ_{-1} separately. We will discuss φ_1. Choosing a smaller, if necessary, we may assume that

$$\max_{\{\|\bar{y}\| \leqq a, \|\bar{\bar{y}}\| = b\}} \|\bar{x}\| < f < \min_{\{\|\bar{y}\| \leqq a, \|\bar{\bar{y}}\| = 1\}} \|\bar{\bar{x}}\| .$$

The "positive" boundaries of w_0 and W_0^+ link $0 \times \mathbb{R}^2$. Since $0 \times \mathbb{R}^2$ is invariant, the same is true for their images. Hence there are constants $0 < e < E$ such that

$$e < \min_{\{\|\bar{y}\| = a, \|\bar{\bar{y}}\| \leqq b\}} \|\bar{x}\| < \max_{\{\|\bar{y}\| = a, \|\bar{\bar{y}}\| \leqq 1\}} \|\bar{x}\| < E.$$

Now let $w_1 = \{\|\bar{x}\| \leqq e, \|\bar{\bar{x}}\| \leqq f\}$ and $w_1 = \{\|\bar{x}\| \leqq E, \|\bar{\bar{x}}\| \leqq f\}$. By means of these choices we have $\varphi_1 : (w_0, \partial_+) \to (W_1, \Delta_+)$ and $\psi_1 : (w_1, \partial_-) \to (W_0^+, \Delta_-)$ as required. Furthermore there are obvious retractions $r_0 : (W_0^+, \Delta_-) \to (w_0, \partial_-)$ and $r_1 : (W_1, \Delta_+) \to (w_1, \partial_+)$ inducting isomorphisms on homology. It remains to verify that φ_1 and ψ_1 induce isomorphism on homology. As we remarked above this can be checked by restricting to the boundaries. ∂_1 is a solid torus linking $0 \times \mathbb{R}^2$ so the same is true of $\varphi_1(\partial_+)$. This shows that φ_{1*} is an isomorphism. ∂_- is a solid torus whose "center" is the square $\|\bar{\bar{x}}\| = c$ in $0 \times \mathbb{R}^2$. For homological purposes we need only consider the effect of ψ_1 on this square. But the ψ_1 image of the square is a simple closed curve in the $\bar{\bar{y}}$ plane encircling the origin so it is linked with $\mathbb{R}^2 \times 0$. This proves that ψ_{1*} is also an isomorphism.

We have now associated to each orbit α in the connection graph three windows in $\tilde{M}$, one in the section Z and one at each end of the orbit in the boundaries of small balls around the restpoints which α connects. Now we will show that if α connects E' to E and β connects E to E' then the windows at the ends of α and β near E are correctly aligned by the perturbed flows. Thus let w_0 be any incoming window at E and w_1 be any outgoing window. In the coordinates of Lemma 3.4 w_0 lies in the $v > 0$ hemisphere of ∂B where B is a ball around E and w_1 lies in the $v = 0$ hemisphere. Both windows are cubes with respect to $(x_1, \ldots, x_4)$ used as coordinates on ∂B near the points where α and β cross it. The auxiliary windows W_0 and W_1 will be tubes around $St(E) \cap \partial B$ and $Un(E) \cap \partial B$ in ∂B, respectively

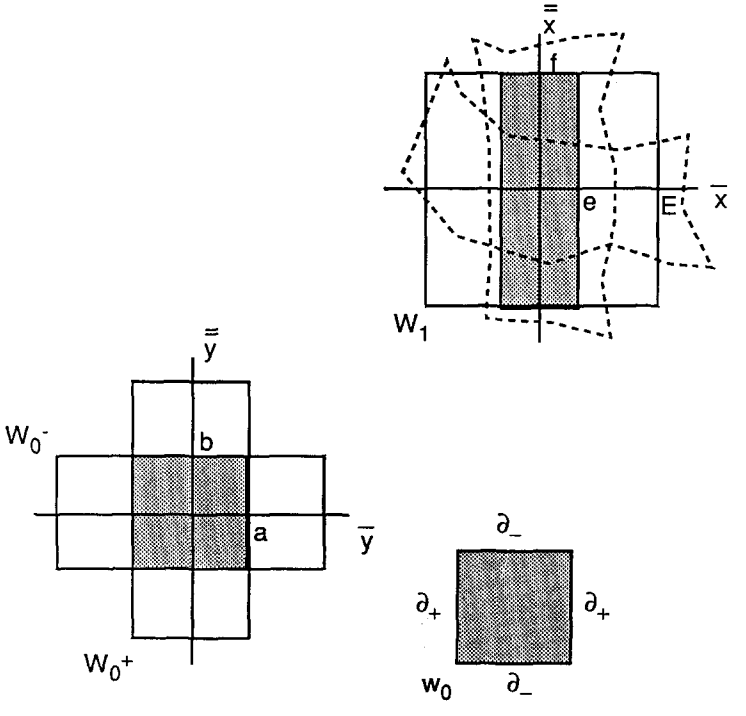

Fig. 12

(see Figure 11). There are obvious retractions $r_0 : W_0 \to w_0$ and $r_1 : W_1 \to w_1$ as required.

First consider what happens to w_0 under the flow on $\tilde{M}$. Every point of w_0 except $q = w_0 \cap St(E)$ leaves B near $Un(E) \cap C$. If W_1 is properly chosen these points will leave through W_1. Points which remain in B for a long time emerge very close to $Un(E)$. Now under perturbation $v' > 0$ so every point of w_0 leaves B and does so near $Un(E) \cap \partial B$. If the perturbation is small enough w_0 will exit B through W_1, *i.e.*, there will be a Poincare map $\varphi : w_0 \to W_1$. Points of ∂_+ leave ∂B near where they did for the unperturbed flow, namely, near $Un(E) \cap C$ so they do not hit w_1. Hence $\varphi : (w_0, \partial_+) \to (W_1, \Delta_+)$. The homology condition of the definition of correct alignment is just that the solid torus $\varphi(\partial_+)$ should link $St(E)$. This was true in $\tilde{M}$ and is still true in $\tilde{M}(h, \omega)$. A similar argument about the backward Poincaré map $\psi : (w_1, \partial_-) \to (W_0, \Delta_-)$ completes the proof of correct alignment:

Proposition 3.5. *Let α and β be connecting orbits represented by edges of the connection graph with a common vertex, E. Let w_0 and w_1 be the windows near E associated to α and β. Then there is a constant $c(\alpha, \beta) > 0$ such that for $0 < |\omega| < c(\alpha, \beta)$, and the flow on $\tilde{M}(h, \omega)$ correctly aligns w_0 and w_1.*

If Γ is any finite subgraph of $G(m, h)$ then we can choose $\omega(\Gamma) > 0$ to be the minimal $c(\alpha, \beta)$ where α, β run over the adjacent edges of Γ. Then Propositions 3.3 and 3.5 imply Theorem 2.

4. Variational Equations and Transversality

In this section we will prove Propositions 2.2 and 2.5 which assert the transversality of certain restpoint connections. In both cases the orbit itself is well understood. For Proposition 2.2 we are considering the branch of the Lagrangian restpoint cycle that lies in the collision set M_0. For Proposition 2.5 we are considering an orbit in the two-dimensional isosceles collision manifold. We prove transversality by studying the variational equations along these orbits.

The variational equations of 1.1 are

$$\begin{bmatrix} \delta r \\ \hline \delta s \\ \hline \delta z \end{bmatrix} = \left[\begin{array}{c|c|c} v & rz^T & rs^T \\ \hline 0 & -vI - sz^T & A^{-1} - ss^T \\ \hline 0 & D\nabla U(s) + \tfrac{1}{2} zz^T & \tfrac{1}{2} vI + \tfrac{1}{2} zs^T \end{array}\right] \begin{bmatrix} \delta r \\ \hline \delta s \\ \hline \delta z \end{bmatrix}$$

where I denotes the 6×6 identity matrix. The tangent space to $M(h, \omega)$ is given by:

$$\begin{gathered} m_1\,\delta s_1 + m_2\,\delta s_2 + m_3\,\delta s_3 = \delta z_1 + \delta z_2 + \delta z_3 = 0, \\ s^T A\,\delta s = 0, \\ z^T A^{-1}\,\delta s - \nabla U(s) \cdot \delta s = h\,\delta r, \\ z^T J\,\delta s - s^T J\,\delta z = 0. \end{gathered} \tag{4.1}$$

We always work with tangent vectors satisfying $\delta r = 0$. If we want to study tangent vectors complementary to the direction of the rotational symmetry we can impose the condition

$$s^T JA\,\delta s = 0. \tag{4.2}$$

Let e be a Lagrangian central configuration. Along the corresponding rest-point cycle we have, as in Section 1, $s(t) = R(\theta(t))\,e$. Then from 1.1 we find

$$z(t) = vAs + \alpha AJs \tag{4.3}$$

where $\alpha = \theta'$. Let P_s be the plane in $T_s\Sigma$ where 4.2 holds and let $AP_s = \{\delta z : \delta z = A\,\delta\hat{s},\ \delta\hat{s} \in P_s\}$. One can show that $P_{R(\theta)s} = P_s$ when both are viewed as subspaces of $\mathbb{R}^6$.

Lemma 4.1. *$P_e \times AP_e = P_{s(t)} \times AP_{s(t)} \subset \mathbb{R}^{12}$ is invariant under the variational equations along the Lagrangian restpoint cycle.*

Proof. The equation follows from the lat remark and the equation $s(t) = R(\theta(t))\,e$. To prove invariance we will differentiate 4.2. First note that if $\delta s \in P_s$ and $\delta z = A\,\delta\hat{s}$, $\delta\hat{s} \in P_s$, then 4.1–4.3 give $s^T\,\delta z = z^T\,\delta s = 0$ so the variational matrix becomes

$$\left[\begin{array}{c|c|c} v & 0 & 0 \\ \hline 0 & -vI & A^{-1} \\ \hline 0 & D\nabla U(s) & \frac{1}{2}vI \end{array}\right]. \tag{4.4}$$

Also $z^T J\,\delta s = s^T J\,\delta z = 0$. From these facts it follows easily that $(s^T JA\,\delta s)' = 0$ and that $(s^T JA(A^{-1}\,\delta z))' = s^T J\,D\,\nabla U(s)\,\delta s$. We will show that this also vanishes. We have $\nabla U(s) \cdot Js = 0$ since this is the derivative of $U(s)$ in the direction of the rotational symmetry. From this we get $s^T J\,D\,\nabla U(s)\,\delta s = \nabla U(S) \cdot J\,\delta s$. Since s is a central configuration and $Js \in T_s\Sigma$, the last expression vanishes. It follows from these facts that $\delta s(t) \in P_{s(t)}$ and $\delta z(t) \in AP_{s(t)}$ for all t.

The variational flow along the restpoint cycle in the quotient manifold $\tilde{M}$ is a linear flow on a five-dimensional bundle. From the lemma it follows that the four-dimensional plane $Pe \times APe$ can be used as an invariant transversal to the direction of the vectorfield along the whole cycle. Hence the study of the variational equations reduce to the time-dependent system induced by 4.4 on $P_e \times AP_e$. Along the branch of the cycle in $\tilde{M}_+$ the equations split further into invariant two-planes. This fact was first observed by DEVANEY and later generalized by SIMO & LLIBRE [D2, S-L]. Along the branch in $\tilde{M}_0$ however this does not generally occur. It does occur for exactly equal masses as we will now show.

In Section 2 we saw that for equal masses the two nontrivial eigenvalues of $D\,\tilde{\nabla}\tilde{U}(s)$ are equal. The eigenvectors lie in P_s. Hence if e_1, e_2 is any basis for P, $D\,\tilde{\nabla}\tilde{U}(s)\,e_j = \lambda e_j$ or $D\,\nabla U(s)\,e_j = (\lambda - U(s))\,Ae_j$ since $\nabla U(s) = A\,\tilde{\nabla}\tilde{U}(s) - U(s)\,A(s)$. If $f_j = Ae_j$ we can use e_1, f_1, e_2, f_2 as a basis for our invariant four-

plane. If a_1, b_1, a_2, b_2 are coordinates with respect to this basis, we find, using 4.4:

$$\begin{bmatrix} a_1 \\ b_1 \\ a_2 \\ b_2 \end{bmatrix} = \left[\begin{array}{cc|cc} -v & 1 & 0 & 0 \\ \hat{\lambda} & \frac{1}{2}v & 0 & 0 \\ \hline 0 & 0 & -v & 1 \\ 0 & 0 & \hat{\lambda} & \frac{1}{2}v \end{array}\right] \left[\begin{array}{c} a_1 \\ b_1 \\ \hline a_2 \\ b_2 \end{array}\right] \tag{4.5}$$

where $\hat{\lambda} = \lambda - U(e)$ and $v(t)$ is computed along the restpoint cycle. When the masses are not equal, one cannot choose a time-independent basis of eigenvectors for $D\tilde{\nabla}\tilde{U}(s(t))$. From Table 1 on 2.2 we have $\lambda = \frac{3}{2}U(e)$ so $\hat{\lambda} = \frac{1}{2}U(e)$. Our considerations are now reduced to the two dimensional system:

$$\begin{bmatrix} a \\ b \end{bmatrix} = \begin{bmatrix} -v(t) & 1 \\ \frac{1}{2}U(e) & \frac{1}{2}v(t) \end{bmatrix} \begin{bmatrix} a \\ b \end{bmatrix}. \tag{4.6}$$

From the equations in Section 1 we find $v' = U(e) - \frac{1}{2}v^2$ along the branch of the restpoint cycle in $\tilde{M}_0$. Now we can prove.

Lemma 4.2. *The cone family* $a(b - \frac{1}{2}va) \geqq 0$ *is positively invariant under equations* 4.6.

Proof. If $a = 0$ then $a' = b$ and $[a(b - \frac{1}{2}va)]' = b^2 \geqq 0$. Hence orbits cannot leave the family through the $a = 0$ boundary. If $b - \frac{1}{2}va$ we find $[a(b - \frac{1}{2}va)]' = \frac{3}{4}v(t)^2 a^2$. This shows that orbits cannot leave through the $b - \frac{1}{2}ba = 0$ boundary either.

This can be used to prove the transversality of the $E^*_{+,-} \to E_{+,-}$ connecting orbits if the masses are equal. Because 4.5 is block diagonal, the tangent spaces to $Un(E^*_{+,-})$ and $St(E_{+,-})$ are direct sums of their intersections with the (a_1, b_1) and (a_2, b_2) planes. These tangent spaces are transverse if and only if their intersections with these coordinate planes are transverse. Now a vector $v \in T_{E^*} Un(E^*) \cap (a_1, b_1)$-plane must lie in the cone family of Lemma 4.2 since it is an attractor in the projective flow on the (a_1, b_1)-plane. Therefore vectors in $T_{(s(t),z(t))} Un(E^*) \cap (a_1, b_1)$-plane lie in the cone family. On the other hand, vectors in $T_{(s(t),z(t))} St(E) \cap (a_1, b_1)$-plane do not lie in the cone family. To see this note that the symmetry $v \to -v$, $\delta s \to \delta s$, $\delta z \to -\delta z$, $t \to -t$ of equations 4.4 takes $T_{E^*} Un(E)$ to $T_E St(E)$. In the (a_1, b_1) plane this reduces to $v \to -v$, $a_1 \to a_1$, $b_1 \to -b_1$. This changes the inequality of Lemma 4.2; hence vectors of $T_E St(E) \cap (a_1, b_1)$-plane do not lie in the cone family. It follows that the same holds for $T_{(s(t),z(t))} St(E)$. We have now shown that $T_{(s,z)} Un(E^*) \cap T_{(s,z)} St(E) \cap (a_j, b_j)$ plane $= \{0\}$ for $j = 1, 2$. Since the full tangent spaces are direct sums, $T_{(s,z)} Un(E^*) \cap T_{(s,z)} St(E) = \{0\}$ as required.

Proposition 2.2 follows from the transversality in the equal mass case since the manifolds $Un(E^*)$ and $St(E)$ depend real analytically on the masses. The set

of masses such that the $E^*_{+,-} \to E_{+,-}$ connections are not transverse will be the zero set of some analytic function of the masses. Since the equal masses do not lie in the zero set, the zero set is at least codimension one.

To prove Proposition 2.5, we assume $m_1 = m_2$ and show that the $E_{+,-} \to C_3$ connection in the isosceles collision manifold is transverse when viewed in the full planar collision manifold. To do this we will find invariant bundles for the variational flow near the isosceles manifold and then find an invariant cone family, as above.

Let $L: \mathbb{R}^6 \to \mathbb{R}^6$ be the linear isometry $L(x_1, y_1, x_2, y_2, x_3, y_3) = (-x_2, y_2, -x_1, y_1, -x_3, y_3)$. This reflects each position vector (x_j, y_j) through the y-axis and then interchanges the first two particles. A fixed point of L is an isosceles configuration: $s = (x, y, -x, y, 0, y_3)$.

Now define $\hat{L}(s, z) = (Ls, Lz)$ and $\hat{L} \times \hat{L}(s, z, \delta s, \delta z) = (Ls, Lz, L\,\delta s, L\,\delta z)$. The fixed points of $\hat{L}$ form a submanifold, $\mathscr{J}$, of M called the isosceles submanifold. Since $m_1 = m_2$, $\hat{L}$ commutes with the flow of 1.1 and so $\mathscr{J}$ is invariant. We will split $T_{\mathscr{J}} M$ into eigenbundles of L. L has eigenvalues ± 1. The $+1$ eigenspace is just $T_{\mathscr{J}} \mathscr{J} = T\mathscr{J}$. The -1 eigenspace we call B. Then $T_{\mathscr{J}} M = T\mathscr{J} \oplus B$ and both bundles are invariant. They are each three-dimensional.

The isosceles collision manifold is $C \cap \mathscr{J}$. We get a splitting $T_{C \cap \mathscr{J}} C = T(C \cap \mathscr{J}) \oplus B_{C \cap \mathscr{J}}$. We will refer to the second factor as just B. Thus $B = \{(s, z, \delta s, \delta z) : (s, z) \in C \cap \mathscr{J},\ (\delta s, \delta z) \in T_{(s,z)} C,\ \hat{L}(\delta s, \delta z) = -(\delta s, \delta z)\}$.

We will introduce a basis in the three-dimensional bundle B. Let $s = (x, y, -x, y, 0, y_3)$ and $z = (\zeta, \eta, -\zeta, \eta, 0, \eta_3)$. Let $e = (1, 0, 1, 0, -2\alpha, 0)$ and $f = (0, 1 + 2\alpha, 0, -(1 + 2\alpha), 0, 0)$ where $\alpha = m_1/m_3 = m_2/m_3$. In the following lemma we indicate the δs and δz components of basis vectors:

Lemma 4.3. *The vectors* $u_1 = (xe + yf, -(m^{-1}\,\zeta Ae + m^{-1}\,\eta Af))$, $u_2 = (0, xAe + yAf)$ *and* $u_3 = (Js, Zz)$ *form a basis for* B *at* $(s, z) \in C \cap \mathscr{J}$.

Proof. The proof consists in checking all the equations defining B on these vectors. We omit the details.

Note that u_3 is just the tangent vector to the action of the rotation group. Thus $\langle u_3 \rangle$ is an invariant one-dimensional bundle of B. To compute the differential equations for the coordinates corresponding to this basis is laborious and we will omit the computation. Expressing vectors in B as $au_1 + bu_2 + cu_3$ we have:

$$\begin{bmatrix} a \\ b \\ c \end{bmatrix}' = \left[\begin{array}{ccc} -2v & 1 & 0 \\ f(s) - 5U(s) & \frac{3}{2} v & 0 \\ \hline * & 0 & 0 \end{array}\right] \begin{bmatrix} a \\ b \\ c \end{bmatrix} \tag{4.7}$$

where $f(s) = (1 + 2\alpha)^{-1} \dfrac{d^2}{dt^2} U(s + t(xe + yf))|_{t=0}$. Since we are really interested in variational equations in the quotient manifold of C under the rotation symmetry, we need only study the first two components of (a, b, c).

Fortunately, the crudest of information about this matrix suffices to show the existence of an invariant cone family. The orbit considered in Prosposition 2.5 is a restpoint connection $E_{+,-} \to C_3$ or $C_3^* \to E_{+,-}^*$. We need to estimate $f(s)$ along this orbit. A direct computation gives

$$f(s) = \frac{2mm_3\beta}{(x^2 + \beta^2 y^2)^{5/2}} [3(x^2 + \beta y^2)^2 - (x^2 + y^2)(x^2 + \beta^2 y^2)].$$

It is easy to see that $f(s) \geqq 0$ when $x^2 \geqq \frac{1}{2}\beta^2 y^2$. Unfortunately we need to consider the range of configurations with $x^2 \geqq \frac{1}{3}\beta^2 y^2$, the equality corresponding to the equilateral configuration. In this case one can at least show $f(s) + U(s) \geq 0$. We will also need to estimate $v(t)$ along the orbit. Since the flow on C is gradient-like with respect to v, $v(t)$ is bounded on either side by its values at the restpoints. It is also true that for the orbits in question $U(s)$ is bounded on either side by its values at the restpoints. From 2.1 we have $v^2 = 2U(s)$ at the restpoints. Since always $v^2 \leqq 2U(s)$ and since $U(e_{-,-}) < U(s)$ we obtain the following estimates:

$$U(e_{-,-}) \leqq U(s) \leqq U(c_3),$$

$$2U(e_{+,-}) \leqq v^2 \leqq 2U(s).$$

A simple computation gives

$$\frac{U(e_{+,-})}{U(c_3)} = \frac{\sqrt{2}\,(2+\alpha)^{3/2}}{(\alpha+4)(1+2\alpha)^{1/2}}. \tag{4.8}$$

Also, if we define s_0 to be the configuration with $x^2 = \frac{1}{2}\beta^2 y^2$, we have

$$\frac{U(e_{+,-})}{U(s_0)} = \frac{\sqrt{6}\,(2+\alpha)^{3/2}}{(3+2\alpha)^{1/2}(\sqrt{3}\alpha+4)}. \tag{4.9}$$

Lemma 4.4. *There exists a positive numner k such that the cone family* $a(b - ka) \geqq 0$ *is invariant under* 4.7.

Proof. In fact we can take $k = \frac{7}{4}\sqrt{2U(e_{-,-})}$. When $a = 0$ we have $[a(b-ka)]' = b^2 \geqq 0$. When $b = ka$ we find:

$$[a(b - ka)]' = a^2[f - 5U + \tfrac{7}{2}vk - k^2].$$

To see that this is nonnegative for $x^2 \geqq \frac{1}{2}\beta^2 y^2$ it suffices to show that

$$-5U(c_3) + \tfrac{49}{8}v\sqrt{2U(e_{+,-})} - \tfrac{49}{8}U(e_{-,-}) \geqq 0.$$

Since $v \geqq \sqrt{2U(e_{+,-})}$,

$$\varrho = \frac{U(e_{-,-})}{U(c_3)} \geqq \frac{40}{49}$$

is good enough. But 4.8 gives $\varrho \geqq \frac{18\sqrt{3}}{7\sqrt{7}}$ which does exceed $\frac{40}{49}$. On the interval $\frac{1}{3}\beta^2 y^2 \leqq x^2 \leqq \frac{1}{2}\beta^2 y^2$, one finds that the following estimate suffices:

$$\hat{\varrho} \equiv \frac{U(e_{+,-})}{U(s_0)} \geqq \frac{48}{49}.$$

From equation 4.9 one can show $\hat{\varrho} \geqq \frac{\sqrt{6}\,(12 - 6\sqrt{3})^{3/2}}{(8 - 3\sqrt{3})^{1/2}(100 - 56\sqrt{3})}$. Incredibly, this exceeds $\frac{48}{49}$!

Now Proposition 2.5 follows from this lemma by the argument used for Proposition 2.2.

Acknowledgments. Research supported by the National Science Foundation and by the Mathematical Sciences Research Institute of Berkeley. This paper is dedicated to the memory of CHARLES CONLEY.

References

[C] C. CONLEY, Invariant sets which carry a one-form, JDE **8** (1970), 587–594.

[D1] ROBERT L. DEVANEY, Triple collision in the planar isosceles three-body problem, Inv. Math. **60** (1980), 249–267.

[D2] ROBERT L. DEVANEY, Structural stability of homothetic solutions of the collinear n-body problem, Cel. Mech. **19** (1979), 391–404.

[E] R. W. EASTON, Isolating blocks and symbolic dynamics, JDE **17** (1975), 98–118.

[Eu] L. EULER, De moto rectilineo trium corporum se mutuo attrahentium, Novi Comm. Acad. Sci. Imp. Petrop. **11** (1767), 144–151.

[L] J. L. LAGRANGE, Oeuvres, vol. 6, 272–292, Paris 1873.

[M1] RICHARD MOECKEL, Heteroclinic phenomena in the isosceles three-body problem, SIAM J. Math. Anal. **15** (1984), 857–876.

[M2] RICHARD MOECKEL, Spiralling invariant manifolds, to appear.

[M3] RICHARD MOECKEL, Orbits near triple collision in the three-body problem, Indiana Univ. Math. Jour. **32** (1983), 221–240.

[M4] RICHARD MOECKEL, Orbits of the three-body problem which pass infinitely close to triple collision, Am. J. Math. **103** (1981), 1,323–1,341.

[Mc1] RICHARD MCGEHEE, Singularities in classical celestial mechanics, Proc. Int. Cong. Math. 827–834, Helsinki, 1978.

[Mc2] RICHARD MCGEHEE, Triple collision in the collinear three-body problem, Inv. Math. **27** (1974), 191–227.

[R-S] C. ROBINSON & D. SAARI, N-body spatial parabolic orbits asymptotic to collinear central configurations, JDE **48** (1983), 434–459.

[S] C. SIMO, Analysis of triple collision in the isosceles problem, in "Classical Mechanics and Dynamical Systems," Maral Dekher, New York, 1980.

[S-L] S. SIMO & J. LLIBRE, Characterization of transversal homothetic solutions in the n-body problem, Arch. Rational Mech. **77**(1981), 189–198.

[S-M] C. SIEGEL & J. MOSER, Lectures on Celestial Mechanics, Springer-Verlag, New York, 1971.

[Sm] S. SMALE, Topology and mechanics I, Inv. Math. **10** (1970), 305–331; II, Inv. Math. **11** (1970), 45–64.

[W] J. WALDVOGEL, The three-body problem near triple collision, Celes. Mech. **14** (1976), 287–300.

School of Mathematics
University of Minnesota-Twin Cities
Minneapolis, Minnesota 55455

(Received July 13, 1988)